

Conductance, magnetoresistance, and interlayer exchange coupling in magnetic tunnel junctions with nonmagnetic metallic spacers and finite thick ferromagnetic layers

Wu-Shou Zhang and Bo-Zang Li

Institute of Physics and Center for Condensed Matter Physics, Chinese Academy of Sciences, P.O. Box 603-99, Beijing 100080, China

Yun Li

Department of Physics, Peking University, Beijing 100871, China

(Received 20 March 1998)

Based on the two-band model and free-electron approximation, magnetism and transport properties of magnetic tunnel junctions with nonmagnetic metallic (NM) spacers and finite thick ferromagnetic (FM) layers are studied. The mean conductance and tunnel magnetoresistance are oscillatory functions of NM and FM thicknesses, their period is determined by the Fermi-surface properties of the metals, and magnetoresistances ($\sim 10^3\%$) much greater than those predicted by Julliere's model are obtained. The oscillation of interlayer exchange coupling with metal layer thickness that originates from the interference of electron waves at different energy levels is found in contrast with the situation in metallic magnetic multilayers. Our results indicate that giant tunnel magnetoresistances with weak antiferromagnetic coupling can be attained by controlling the metal layer thickness, and this has potential in designing spin-polarized tunneling devices.

[S0163-1829(98)03346-3]

I. INTRODUCTION

Since the discovery of the giant magnetoresistance (GMR) in metallic magnetic multilayers (MMM's),¹ there has been a renewed interest in the phenomenon of the tunnel magnetoresistance (TMR) in magnetic tunnel junctions (MTJ's) consisting of two ferromagnetic (FM) electrodes separated by a tunneling barrier (insulator or semiconductor) layer [FM/I(S)/FM].^{2,3} More recently, large TMR's were achieved in FM/I/FM structures⁴⁻⁸ which render MTJ's more promising than MMM's in the manufacture of magnetic-field sensors and digital storage devices. Since the resistance and field sensitivity of MTJ's are much higher than those of MMM's, the power consumed and magnetic field needed will be much less.

Julliere² discussed the TMR effects using Tedrow and Meservey's analysis,⁹ and he showed that TMR is proportional to the spin-polarization factors of two FM's. Slonczewski¹⁰ studied MTJ's based on the free-electron approximation by analyzing the transmission of charge and spin current through a rectangular barrier separating two semi-infinite free-electron-like FM's. He predicted that the tunnel conductance varies as the cosine of the relative angle of two FM's magnetizations and it was verified widely,^{4,5,11} and TMR depends not only on the spin-polarization factors of FM's as that of Julliere but also on the barrier height. MacLaren *et al.*¹² verified that Slonczewski's model provides a good approximation to the exact expressions for free electrons in the limit of thick barrier. Besides these two models, there were other theories had been applied to the system.¹³⁻¹⁸

Another extensively studied subject in MMM's and MTJ's is the interlayer exchange coupling (IEC). It is found that IEC oscillates in sign with the nonmagnetic metallic (NM) thickness in MMM's,^{19,20} and this effect can be de-

scribed in terms of the Ruderman-Kittel-Kasuya-Yosida theory,²¹ or quantum well theory.²² IEC also changes as a function of FM thickness as predicted theoretically^{23,24} and later observed experimentally.^{25,26} As concerns theories about IEC in MTJ's, two models have been proposed: One is the so-called free-electron model due to Slonczewski as mentioned above.¹⁰ It predicts antiferromagnetic (AF) coupling for low barrier height and ferromagnetic (FM) coupling for high barrier height, and the strength of IEC decreases exponentially with the barrier thickness; The other model is due to Bruno.²⁷ By using the t -matrix formalism, the coupling is expressed in terms of the spin asymmetry of the reflection at the I(S)/FM interfaces. It succeeds in obtaining an IEC coupling which increases with temperature, and it reduces to Slonczewski's results at zero temperature.

Recently, Vedyayev *et al.*²⁸ and the present authors²⁹ studied MTJ's with NM spacers between the FM's and barrier, i.e., FM/NM/I(S)/FM [and/or FM/NM/I(S)/NM/FM]. The results showed that the presence of thin NM spacers can lead to the formation of quantum well states that lead to oscillations of TMR and IEC in sign with NM thickness. TMR values much greater than those in the conventional sandwiched MTJ's with low AF coupling can be obtained in the structure.

Based on the previous results we study a more realistic MTJ with NM spacers and finite thick FM layers in this work. It is found that the mean conductance and TMR oscillate with the NM and FM thicknesses, but the oscillation of IEC with these thicknesses exhibits multiple periods which are similar to those in MMM's but have different physical origins.

The plan of the paper is as follows. In Sec. II, the model Hamiltonian is established and the corresponding Schrödinger equation is solved, then we give the analytical and numerical results of conductance and TMR in Sec. III, IEC in Sec. IV. At last, we discuss the related topics about this

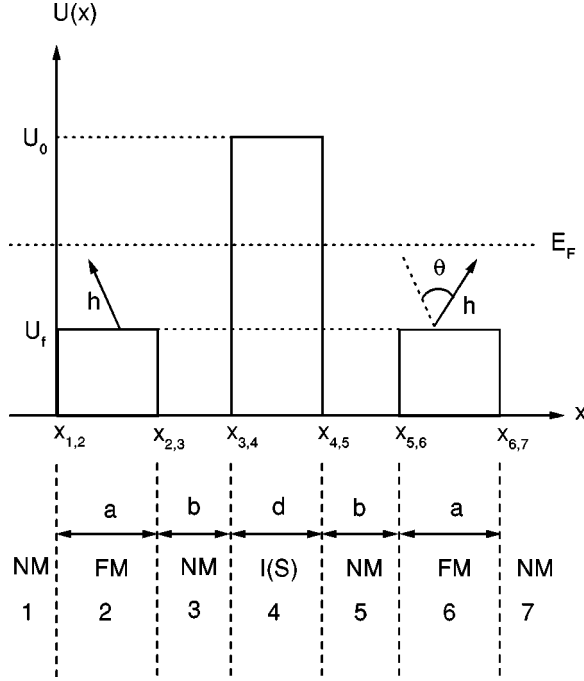


FIG. 1. Schematic potential for NM/FM/NM/I(S)/NM/FM/NM junction. U_f and U_0 are the crystalline potentials in the FM and barrier layers, respectively; \mathbf{h} is the molecular field of the FM's; θ is the angle between magnetization of two FM's; a , b , and d are the thicknesses of the FM, NM, and barrier layers, respectively.

model (Sec. V) and conclude the paper with a summary (Sec. VI).

II. MODEL

Consider two single-domain transition FM's separated by two flat plane NM's plus a flat plane tunneling barrier and covered on both sides by two semi-infinite NM cap layers as lead wires (see Fig. 1). For simplicity, we assume that the FM's are made of the same metal and have the same thickness a , the NM spacers and cap layers are made of the same material and the spacers have the same thickness b . This assumption, however, can be released easily without changing qualitatively the physical behavior of system. a , b and the barrier thickness d , are much smaller than their in-plane dimensions so that the system may be considered as homogeneous in the yz plane (parallel to the interfaces) and inhomogeneous only in the x direction (growth direction). Within each layer, the electrons are described as a free-electron gas.^{10,12,28-32} Between layers, they experience potential steps. The latter are spin dependent at the FM/NM interfaces ($x = x_{1,2}$, $x_{2,3}$, $x_{5,6}$, and $x_{6,7}$) due to the exchange splitting of the d band in the FM's. In contrast, the height of the energy barrier is spin independent at the NM/I(S) interfaces ($x = x_{3,4}$ and $x_{4,5}$). In the present model, no diffuse scattering is introduced at the interfaces and in each layer. The profile of energy seen by the conduction electrons can be represented as drawn in Fig. 1. By assumption of small external voltage, the longitudinal (along the x direction) part of the effective one-electron Hamiltonian takes the following form:

$$H = -\frac{\hbar^2}{2m_i^*} \frac{d^2}{dx^2} + U(x) - \mathbf{h}(x) \cdot \boldsymbol{\sigma}, \quad (1)$$

where m_i^* ($i = 1-7$) is the electron effective mass in region i . In practice, m_i^* may differ from the mass of free electron, for simplicity, we assume all electrons have the same mass m as that of the free electron. $U(x)$ is the potential which is uniform in each layer, $-\mathbf{h}(x) \cdot \boldsymbol{\sigma}$ is the internal exchange energy with $-\mathbf{h}(x)$ denoting the molecular field and $\boldsymbol{\sigma}$ being the conventional Pauli spin operator. Although transverse momentum $\hbar k_{\parallel}$ is omitted from the above notations, the effects of summation over k_{\parallel} will be accounted for in our results.

Corresponding to the Hamiltonian in Eq. (1), all components of eigenspinors of H with eigenenergy E are of the plane-wave form, the wave vector (or virtual wave vector) in each region is

$$\begin{cases} k_n = \frac{1}{\hbar} \sqrt{2mE}, & \text{for NM,} \\ k_{\sigma} = \frac{1}{\hbar} \sqrt{2m(E - U_f + \sigma h)}, & \text{for FM,} \\ i\kappa = \frac{1}{\hbar} \sqrt{2m(E - U_0)}, & \text{for barrier,} \end{cases} \quad (2)$$

where the subscript n indicates the NM layer; $\sigma = \pm 1$ correspond to $\sigma = \uparrow, \downarrow$ (the majority- and minority-spin electrons); U_f and U_0 are the crystalline potentials in the FM's and barrier relative to NM, respectively; h is the amplitude of $\mathbf{h}(x)$ in the FM's and is constant; the directions of \mathbf{h} , hence the corresponding spin quantization axes, differ by the angle θ between the two FM layers (see Fig. 1).

Consider a spin-up incident plane wave having unit particle flux in region 1 (NM electrode, $x < x_{1,2}$ in Fig. 1), the eigenfunction of H in each region is

$$\begin{aligned} \psi_{1\uparrow} &= k_n^{-1/2} e^{ik_n(x-x_{1,2})} + R_{1\uparrow} e^{-ik_n(x-x_{1,2})}, \\ \psi_{1\downarrow} &= R_{1\downarrow} e^{-ik_n(x-x_{1,2})}, \\ \psi_{i\sigma} &= L_{i\sigma} e^{ik_{i\sigma}(x-x_{i-1,i})} + R_{i\sigma} e^{-ik_{i\sigma}(x-x_{i-1,i})}, \quad i = 2-6, \\ \psi_{7\sigma} &= L_{7\sigma} e^{ik_n(x-x_{6,7})}, \end{aligned} \quad (3)$$

where $L_{i\sigma}$ and $R_{i\sigma}$ ($i = 1-7$, $\sigma = \uparrow, \downarrow$) are coefficients to be determined, the index i denotes region i , $k_{i\sigma}$ is a wave vector given in Eq. (2), $x_{i-1,i}$ is the coordinate of boundary between region $i-1$ and i .

To complete the solution of the Schrödinger equation, one must find the 24 unknowns by matching ψ_{σ} and $d\psi_{\sigma}/dx$ at the interfaces $x = x_{i-1,i}$, ($i = 2-5, 7$). The change in quantization axis at $x = x_{5,6}$ requires the spinor transformation

$$\begin{aligned} \psi_{5\uparrow} &= \psi_{6\uparrow} \cos\left(\frac{\theta}{2}\right) + \psi_{6\downarrow} \sin\left(\frac{\theta}{2}\right), \\ \psi_{5\downarrow} &= \psi_{6\downarrow} \cos\left(\frac{\theta}{2}\right) - \psi_{6\uparrow} \sin\left(\frac{\theta}{2}\right), \end{aligned} \quad (4)$$

and similarly for their derivatives.

Some algebra produces the approximate solution for $L_{i\sigma}$ and $R_{i\sigma}$ that is accurate to leading order in $e^{-\kappa d}$. For simplicity, we give only $L_{7\sigma}$

$$L_{7\uparrow} = 4D_{\uparrow}^2 e^{-\kappa d} k_n^{5/2} \kappa \cos\left(\frac{\theta}{2}\right),$$

$$L_{7\downarrow} = 4D_{\uparrow} D_{\downarrow} e^{-\kappa d} k_n^{5/2} \kappa \sin\left(\frac{\theta}{2}\right) \quad (5)$$

with

$$D_{\sigma} = \frac{k_{\sigma}(k_{\sigma} \cos \alpha_{\sigma} + i k_n \sin \alpha_{\sigma})}{[\kappa^2 + k_n^2]^{1/2} [f_{\sigma}(\beta)]^{1/2} f_{\sigma}(\alpha_{\sigma})} \quad \text{for } E > U_f + h, \quad (6)$$

$$f_{\sigma}(x) = k_n^2 \sin^2 x + k_{\sigma}^2 \cos^2 x, \quad (7)$$

$$\beta = k_n b - \arctan(\kappa/k_n), \quad (8)$$

and

$$\alpha_{\sigma} = k_{\sigma} a - \arctan\left(\frac{k_{\sigma}}{k_n} \cot \beta\right). \quad (9)$$

The expression of other coefficients is tedious so we omitted it here and it can be obtained by the continuity conditions at the boundaries.

In the following two sections, we will evaluate the tunnel conductance, TMR, and IEC within the barrier region ($x_{3,4} \leq x \leq x_{4,5}$) where $h=0$. In addition, we will consider only the case of the two-band model for the density of states and zero temperature as done in Refs. 10 and 29–31.

III. CONDUCTANCE AND TUNNEL MAGNETORESISTANCE

The particle transmissivity of majority-spin incident electrons is

$$T_{\uparrow} = \text{Im} \sum_{\sigma} \psi_{\sigma}^* \frac{d\psi_{\sigma}}{dx}. \quad (10)$$

The particle transmissivity of minority-spin incident electrons, T_{\downarrow} is given by the same expression with k_{\uparrow} and k_{\downarrow} interchanged. The summation of $-e(T_{\uparrow} + T_{\downarrow})/2$ over occupied states gives the total charge current (I_e) per unit flowing from region 1 to 7. The differential tunnel conductance G is defined as $G = dI_e/dV$. The detailed procedure for calculating G can be found in Ref. 33.

At zero temperature and small applied voltage, for nearly normal incidence, electrons with E_x near E_F should carry most of the current, so that we can replace E_x with E_F in calculating the conductance due to tunneling. By summing the charge transmission over E_x and k_{\parallel} for occupied states in the usual manner,^{10,12,28–31,33} one finds the conventional expression

$$G = \frac{e^2 \kappa}{8 \pi^2 \hbar d} (T_{\uparrow} + T_{\downarrow})|_{E=E_F}. \quad (11)$$

Some algebra produces the area conductance as

$$G = \bar{G} (1 + \varepsilon \cos \theta), \quad (12)$$

where the mean conductance is

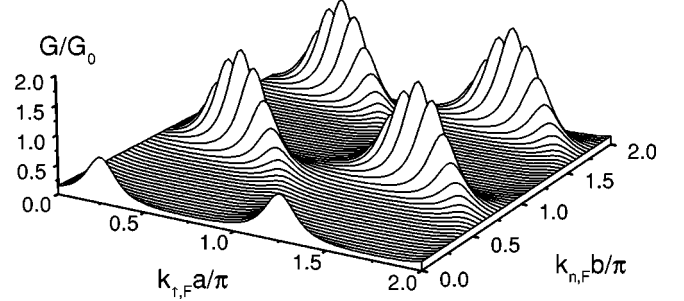


FIG. 2. The mean tunnel conductance \bar{G} as a function of the reduced FM thickness, $k_{\uparrow,F} a/\pi$ and NM thickness, $k_{n,F} b/\pi$. \bar{G} has been normalized to 1 by division $\bar{G}_0 = e^2 \exp(-2\kappa d)/\hbar d^2$. The parameters: $k_{n,F} = k_{\downarrow,F} = 0.4 k_{\uparrow,F}$, $\kappa_F = k_{\uparrow,F}$, $\kappa_F d = 3$.

$$\bar{G} = \frac{e^2 \kappa^3 k_n^6}{\pi^2 \hbar d} e^{-2\kappa d} (|D_{\uparrow}|^2 + |D_{\downarrow}|^2)|_{E=E_F}, \quad (13)$$

and the TMR ratio is defined as

$$R_{\text{TMR}} = \frac{G_{\uparrow\uparrow} - G_{\uparrow\downarrow}}{G_{\uparrow\downarrow}} = \frac{2\varepsilon}{1 - \varepsilon} = \frac{(1 - X)^2}{2X}|_{E=E_F}, \quad (14)$$

where

$$X = \frac{|D_{\uparrow}|^2}{|D_{\downarrow}|^2} = \frac{k_{\uparrow}^2 f_{\downarrow}(\beta) f_{\downarrow}(\alpha_{\downarrow})}{k_{\downarrow}^2 f_{\uparrow}(\beta) f_{\uparrow}(\alpha_{\uparrow})} \quad (15)$$

with $f_{\sigma}(x)$, β , and α_{σ} being the same as those in Eqs. (7)–(9). Figures 2 and 3 show \bar{G} and R_{TMR} as functions of a and b , the FM and NM thicknesses. We find they oscillate with a and b , and the period is determined by the Fermi wave vectors. Another remarkable feature is that R_{TMR} can be much greater than that observed in past experiments and predicted by conventional theories.^{2,10} Based on Julliere's and Slonczewski's models, $R_{\text{TMR}} \leq 2P^2/(1 - P^2) = (k_{\uparrow,F} - k_{\downarrow,F})^2/2k_{\uparrow,F}k_{\downarrow,F} = 45\%$ (P is spin-polarization factor of FM's) for parameters given in Fig. 2 ($k_{\downarrow,F} = 0.4k_{\uparrow,F}$), but the present MTJ's exhibit the maximum R_{TMR} up to 220%. This means that we can obtain an enhanced TMR ratio using the present structure.

The results in Figs. 2 and 3 show a special case, i.e., $k_{n,F} = k_{\downarrow,F}$ ($U_f = -h_0$, e.g., Fe/Cr). The minority electrons are free in regions of FM and NM, $f_{\downarrow}(x) = k_n^2$ in Eq. (7) so the oscillatory period, $T_{\text{FM}} = \pi/k_{\uparrow,F}$. Another special case is $k_{n,F} = k_{\uparrow,F}$ ($U_f = h_0$, e.g., Co/Cu), in which $T_{\text{FM}} = \pi/k_{\downarrow,F}$.

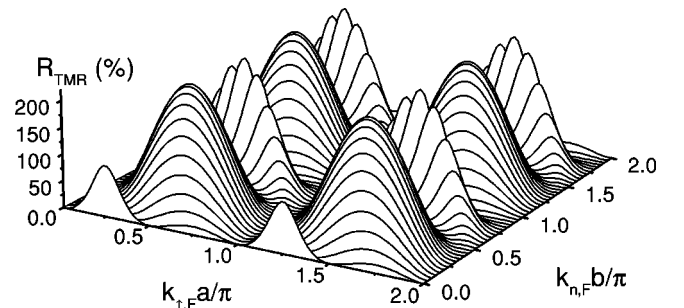


FIG. 3. TMR as a function of $k_{\uparrow,F} a/\pi$ and $k_{n,F} b/\pi$. The parameters are the same as those in Fig. 2.

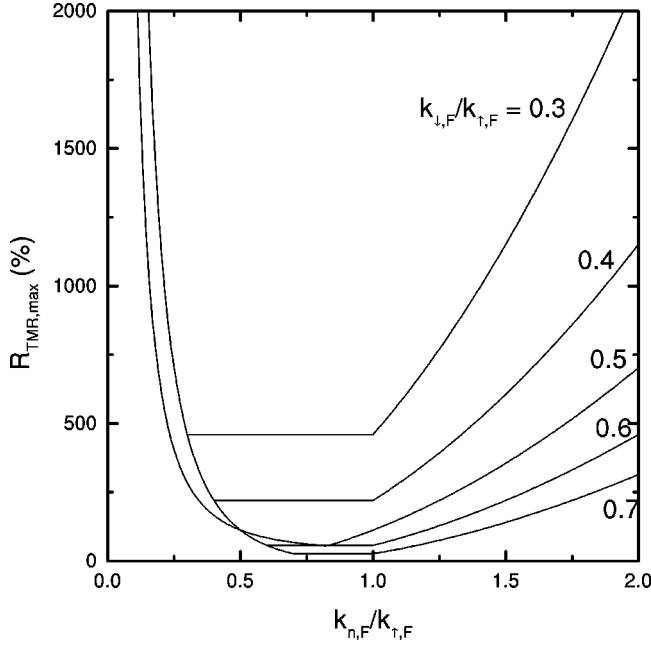


FIG. 4. Maximum TMR vs $k_{n,F}/k_{\uparrow,F}$ for different values of $k_{\downarrow,F}/k_{\uparrow,F}$ as shown beside each curve.

Other situations are complex with T_{FM} determined by the lowest common multiple of period for majority and minority electrons, i.e., $T_{\text{FM}} = [\pi/k_{\uparrow,F}, \pi/k_{\downarrow,F}]$. Suppose the FM's in Figs. 2 and 3 are Fe, we have $k_{\uparrow,F} = 1.09 \text{ \AA}^{-1}$ (Ref. 32) and $T_{\text{FM}} = 2.88 \text{ \AA}$. The lattice constant for α -Fe is 2.86 \AA , verifying that T_{FM} is about the interatomic spacing and this case is similar to the aliasing effect in the oscillatory coupling through NM spacers in MMM's. It can lead to a measured period that is significantly longer than the theoretical one. The effective period can be expressed as: $T_{\text{FM,eff}} = 2/|1/T_{\text{FM}} - 2n/c|$ where c is the monolayer thickness of FM, n is chosen such that $T_{\text{FM,eff}} > 2c$.²¹

The oscillatory period with b determined by $k_{n,F}$ as shown in Figs. 2, 3 and the previous results.^{28,29} The aliasing effect is similar to the above discussion.

In contrast to that of the conventional sandwiched MTJ's, we find the height of barrier has no effect on the amplitude except the phase of R_{TMR} vs a and b as indicated by Eqs. (7)–(9), (14), and (15). We assume that m_i^* in Eq. (1) is the same as the free-electron mass m . Although m^* may be different from m (obviously so in an insulator) and it affects TMR in conventional MTJ's,¹³ it has little effect in the present model. This is because the influence of effective mass can transfer to the effective barrier height.

Because R_{TMR} is the oscillatory function of a and b , it is interesting to obtain the maximum R_{TMR} , $R_{\text{TMR,max}}$ for given parameters. We find if $k_{\downarrow,F}/k_{\uparrow,F} \neq 1/2$, when

$$X = \frac{\min^2(k_n, k_{\downarrow})}{\max^2(k_n, k_{\uparrow})} = \begin{cases} k_n^2/k_{\uparrow}^2, & k_{n,F} \leq k_{\downarrow,F}, \\ k_{\downarrow}^2/k_{\uparrow}^2, & k_{\downarrow,F} \leq k_{n,F} \leq k_{\uparrow,F}, \\ k_{\uparrow}^2/k_n^2, & k_{\uparrow,F} \leq k_{n,F}, \end{cases} \quad (16)$$

there will be $R_{\text{TMR,max}}$ as shown in Fig. 4. For fixed $k_{n,F}/k_{\uparrow,F}$, if $k_{\downarrow,F} \leq k_{n,F}$, a lower $k_{\downarrow,F}/k_{\uparrow,F}$ (higher spin-polarization factor) results in a higher $R_{\text{TMR,max}}$ as expected,

but if $k_{\downarrow,F} \geq k_{n,F}$, it has no effect on $R_{\text{TMR,max}}$. For fixed $k_{\downarrow,F}/k_{\uparrow,F}$, if $k_{\downarrow,F} \leq k_{n,F} \leq k_{\uparrow,F}$, $R_{\text{TMR,max}}$ does not change with $k_{n,F}/k_{\uparrow,F}$; Otherwise, $R_{\text{TMR,max}}$ decreases with $k_{n,F}/k_{\uparrow,F}$ when $k_{n,F} < k_{\downarrow,F}$ but increases when $k_{n,F} > k_{\uparrow,F}$. This means we can choose a suitable NM material to enhance R_{TMR} regardless the type of FM. But in the conventional MTJ's, only a FM with great polarization factor (e.g., Fe) will give greater R_{TMR} than that with lower one (e.g., Ni).

Another special case is for $k_{\downarrow,F}/k_{\uparrow,F} = 1/2$, there is

$$X = \begin{cases} \frac{k_{\uparrow}^2 k_n^2 + k_{\downarrow}^2}{k_{\downarrow}^2 2k_n^2}, & k_{n,F} \leq \sqrt{\frac{1+\sqrt{3}}{4}} k_{\uparrow,F}, \\ k_{\downarrow}^2/k_n^2, & \sqrt{\frac{1+\sqrt{3}}{4}} k_{\uparrow,F} \leq k_{n,F} \end{cases}, \quad (17)$$

that corresponds to $R_{\text{TMR,max}}$ as shown in Fig. 4, too. Equations (14), (16), (17), and the related Fig. 4 give the upper limit of TMR ratios which are much greater than those in conventional structures.

IV. INTERLAYER EXCHANGE COUPLING

Slonczewski introduced and employed a method for calculating exchange coupling from torque produced by rotation of the magnetization of one FM to that of the other.¹⁰ This method was further elaborated by Erickson *et al.*,³⁴ Edwards *et al.*³⁵ and Drchal *et al.*³⁶ This method of calculating the torque involves the construction of a spin-flip or exchange current, which is a measure of the probability that an incident electron will undergo a change of spin state on transmission through the NM spacers and barrier layer. The spin-flip current due to a majority-spin electron of energy E incident from the left electrode, j_e^{\uparrow} is expressed as

$$j_e^{\uparrow} = \frac{\hbar}{2m} \text{Re}(\psi_{\downarrow}^* \psi_{\uparrow}' - \psi_{\uparrow}^* \psi_{\downarrow}'). \quad (18)$$

Similarly, one obtains the current due to a minority-spin electron incident from the left electrode, j_e^{\downarrow} by applying this equation with k_{\uparrow} and k_{\downarrow} interchanged. The net current of majority- and minority-spin electrons j_T is calculated by summing both j_e^{\uparrow} and j_e^{\downarrow} over allowed states up to the Fermi energy, then multiplying by a factor of 2 to account for electrons incident from the right NM electrode, which contribute equally to the total spin current

$$j_T = 2 \sum_{0 < E < E_F} (j_e^{\uparrow} + j_e^{\downarrow}). \quad (19)$$

The coupling strength J of the Heisenberg term ($J > 0$ is for FM coupling) is given by

$$J = -\hbar j_T / 2 \sin \theta. \quad (20)$$

After some algebra, we have

$$J = \frac{2m}{\pi^2 \hbar^2} \sum_{\sigma} \int_0^{E_F} k_n^6 \kappa^2 \exp(-2\kappa d) |D_{\sigma}|^2 \text{Im}(D_{\sigma} D_{-\sigma}^*) \times (E_F - E) dE \quad (21)$$

$$= \frac{2m}{\pi^2 \hbar^2} \int_0^{E_F} k_n^6 \kappa^2 \exp(-2\kappa d) (|D_{\uparrow}|^2 - |D_{\downarrow}|^2) \text{Im}(D_{\uparrow} D_{\downarrow}^*) \times (E_F - E) dE \quad (22)$$

$$|D_{\sigma}|^2 = \frac{k_{\sigma}^2}{(\kappa^2 + k_n^2) f_{\sigma}(\beta) f_{\sigma}(\alpha_{\sigma})}, \quad (23)$$

with

and

$$\text{Im}(D_{\uparrow} D_{\downarrow}^*) = \frac{k_n k_{\uparrow} k_{\downarrow} [(k_{\uparrow} + k_{\downarrow}) \sin(\alpha_{\uparrow} - \alpha_{\downarrow}) - (k_{\uparrow} - k_{\downarrow}) \sin(\alpha_{\uparrow} + \alpha_{\downarrow})]}{2(\kappa^2 + k_n^2) [f_{\uparrow}(\beta) f_{\downarrow}(\beta)]^{1/2} f_{\uparrow}(\alpha_{\uparrow}) f_{\downarrow}(\alpha_{\downarrow})} \quad (24)$$

for $E > U_f + h$, where $f_{\sigma}(x)$, α_{σ} , and β are the same as those in Eqs. (7)–(9). IEC consists of two components, one including $|D_{\uparrow}|^2$ is for the majority-spin flip current and the counter one is for the minority-spin flip current.

Numerical results of IEC are shown in Figs. 5–8, changes of J with a and b have features of decaying oscillations as those in MMM's but the amplitude is smaller by a factor $\exp(-2\kappa_f d)$ than the latter.^{10,29} Another interesting feature is the multiple period of oscillation. From Eqs. (21)–(24), we find that different E results in different k_{σ} and k_n , hence there is different period of oscillation with a and b . Because electron waves with different energy levels all contribute to J , summation of different period oscillations results in multiple period. This is in contrast to IEC in MMM's where different energy states contribute to oscillation of different periods, but most of them cancel each other out and only the states near the Fermi level have the most contribution. IEC in MMM's embodies properties of the Fermi surface such as GMR, and transport and magnetic properties are correlated with each other.³⁷ There are also multiple periods of IEC

with metal layer thickness in MMM's that originate from the specific shape of Fermi surface^{21,38} but they are not an effect of the total energy.

For simplicity, we discuss two special situations: One is $k_{n,F} = k_{\downarrow,F}(U_f = -h_0)$, e.g., Fe/Cr as illustrated in Figs. 5 and 6. Figure 5 shows J as a function of a while b is fixed, it exhibits multiple periods as discussed above. Because $f_{\downarrow}(x) = k_n^2$ and $|D_{\downarrow}|^2 = 1/k_n^2(\kappa^2 + k_n^2)$, the oscillatory part mainly comes from the majority-spin flip current, while the minority-spin flip current has a small contribution to it. The oscillatory behavior of J vs b appears clearly in Fig. 6. The striking difference with the oscillation of J vs a is that the oscillations are not necessarily around zero; instead, J may oscillate around a positive, zero, or negative value, depending on the choice of a . This is an important consequence for the experimental observation the oscillatory behavior of J vs b . If one uses a technique that is sensitive only to the sign of coupling, then it is necessary to choose properly the FM thickness, so that the oscillations do actually yield a change of sign of J . This property can be understood from Eqs.

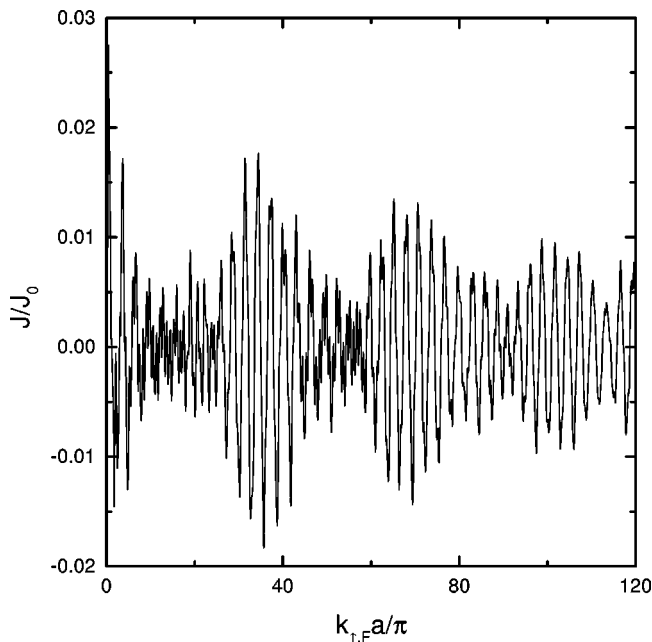


FIG. 5. IEC as a function of $k_{\uparrow,F} a / \pi$ for $k_{n,F} b / \pi = 5$. J has been normalized to 1 by division $J_0 = 2m E_F^2 \exp(-2\kappa d) / \pi^2 \hbar^2$. The other parameters are the same as those in Fig. 2.

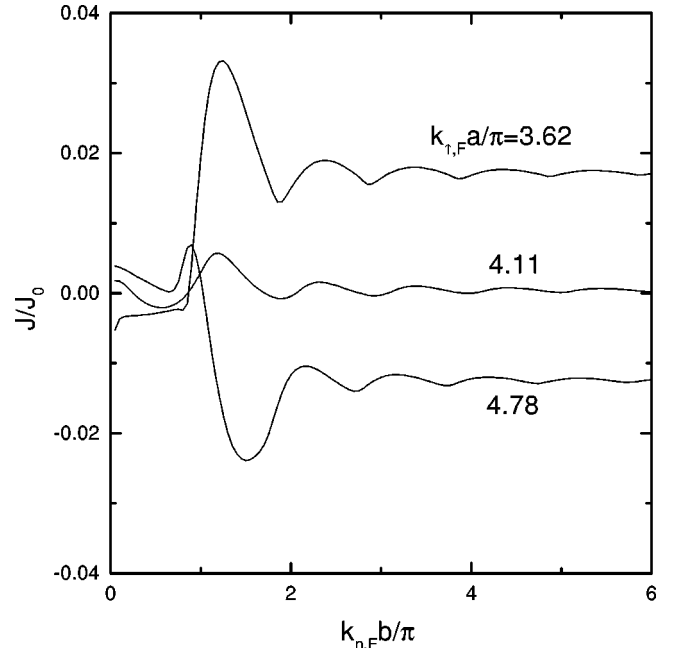


FIG. 6. IEC as a function of $k_{n,F} b / \pi$ for various values of $k_{\uparrow,F} / k_{\downarrow,F}$ as shown beside each curve. The parameters are the same as those in Fig. 5.

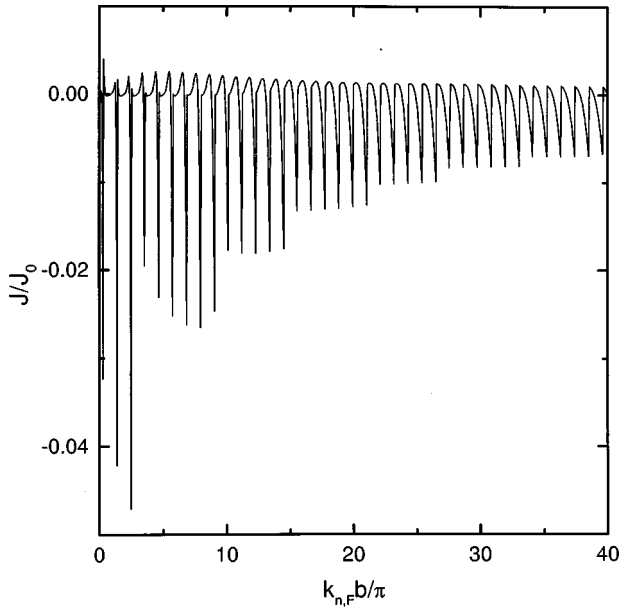


FIG. 7. IEC as a function of $k_{n,F}b/\pi$ for $k_{\uparrow,F}a/\pi=5.5$. The parameters: $k_{n,F}=k_{\uparrow,F}$, $k_{\downarrow,F}=0.4 k_{\uparrow,F}$, $\kappa_F=k_{\uparrow,F}$, $\kappa_F d=3$.

(21)–(24), because $f_{\uparrow}(\beta) > 0$, J does not oscillate in sign with b but its asymptotic value is determined by a .

Another special case is $k_{n,F}=k_{\uparrow,F}$ ($U_f=h_0$, e.g., Co/Cu) as shown in Figs. 7 and 8. When $E < U_f+h$ the minority electrons face barriers at NM/FM interfaces, so there is an exponential decaying factor $\exp(-|k_{\downarrow}|a)$ in the factor $\text{Im}(D_{\uparrow}D_{\downarrow}^*)$ in the integrand of Eq. (22). It means that electrons with energy $E < U_f+h$ have no significant contribution to J beyond a few FM monolayers. We need only pay attention to the energy region of $U_f+h < E < E_F$. When E is near U_f+h , $k_n \gg k_{\downarrow}$, there is $f_{\uparrow}(x) \approx k_n^2 \sin^2 x$, i.e., $|D_{\downarrow}|^2 \propto \csc^2 \beta \csc^2 \alpha_{\downarrow}$ while $|D_{\uparrow}|^2 = 1/k_n^2(\kappa^2 + k_n^2)$, so the minority-

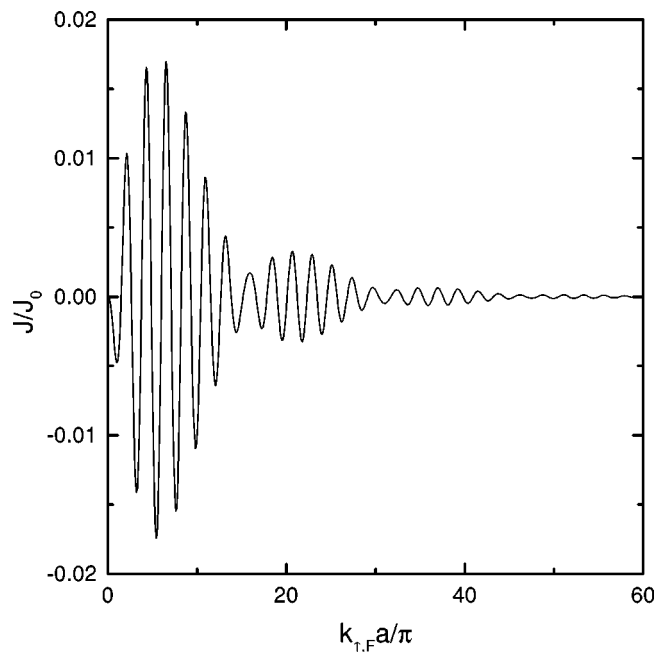


FIG. 8. IEC as a function of $k_{\uparrow,F}a/\pi$ for $k_{n,F}b/\pi=9$. The other parameters are the same as those in Fig. 7.

spin flip current gives most of the contribution to IEC. Figure 7 shows J vs b for a fixed, and illustrates that the sharp peaks come from the electrons which satisfy the resonant condition, $\beta = n\pi$. As b increases, the number of energy levels which satisfy the resonant condition increases and the peaks widen correspondingly. Figure 7 shows the AF coupling and it can also exhibit the FM coupling if other values of a are chosen. Figure 8 illustrates J vs a with fixed b and it also manifests the multiple periods as discussed above.

In realistic MTJ's, $k_{n,F}$ is not necessarily equal to $k_{\uparrow,F}$ or $k_{\downarrow,F}$, but according to the above discussion we conclude that (1) the electrons with energy $U_f+h < E < E_F$ all give their contribution to IEC, and the summation of different states gives the multiple periods of oscillation of J with a and b ; (2) if $k_{n,F} < k_{\uparrow,F}$ ($U_f < h$), J approaches a constant as b increases; (3) if $k_{n,F} \geq k_{\uparrow,F}$ ($U_f \geq h$), J exhibits sharp peaks at some thicknesses of FM and NM.

V. DISCUSSION

We point out that the electrons with momentum perpendicular to the interface give the largest contribution to the TMR due to the strong decrease of the factor $\exp(-2\kappa d)$ with x . This one-dimensional character of transport through the tunneling barrier leads to quite sharp resonances in conductivity. It is in contrast with MMM's in which quantum size effects on the conductivity also exist but lead to much smoother oscillations due to the averaging of all incidences of conduction electrons. The predicted sharp resonance may be difficult to observe experimentally. Indeed, the roughness of the layers leads to spatial fluctuations in the thickness of the FM, NM, and barrier layers. If the roughness is smaller than the Fermi wavelength, it may be taken into account by averaging the currents over a distribution of thickness with an amplitude of one or several monolayers. Even in that case, the averaged value of TMR in the present MTJ is larger than that for the ordinary MTJ of the sandwiched structure.

The present results are appropriate only to the case $a, b \leq \text{MPF}$ (mean free path of electrons), otherwise the electrons will be scattered in FM's and NM's and the quantum size effect will be destroyed. If $a > \text{MPF}$, the effects of reflection on the outer FM/NM interfaces ($x_{1,2}, x_{6,7}$) can be omitted and the present structure will be identical to the FM/NM/I(S)/NM/FM structure as discussed before.^{28,29} If $b > \text{MPF}$, the electrons will lose the polarization memory and the present structure reduces to a normal tunnel junction.

The preceding elementary model does not take into account the generally important complications such as interfacial roughness, electron-electron correlations,¹⁴ bias^{5,15,16} and temperature¹⁴ dependence, and spin-flip tunneling.¹⁷ However, it does provide a basis for initial appraisal of magnetic and transport effects on MTJ's arising from NM spacers and finite thick FM layers. Although not verified at present, our results indicate that we can alter TMR and IEC, and obtain giant TMR ratios with lower IEC in the MTJ's by controlling the FM and NM thicknesses.

VI. SUMMARY

We have studied the magnetism and transport properties of MTJ with NM spacers and finite thick FM layers. It is

found that the mean conductance and TMR are oscillatory functions of the FM and NM thicknesses, and the oscillation of IEC with these thicknesses exhibit multiple periods. Giant TMR with weak AF coupling can be obtained in the mixed structure and it has potential in designing spin-polarized tunneling sensors with a large TMR and field sensitivity.

ACKNOWLEDGMENTS

We would like to express sincere thanks to Professor Fu-Cho Pu and Dr. Jun-Zhong Wang for helpful discussion. This work was supported by the Natural Science Foundation in China under Grants No. 19774076 and 59392800.

- ¹M. N. Baibich, J. M. Broto, A. Fert, F. Nguyen Van Dau, F. Petroff, P. Etienne, G. Creuzet, A. Friederich, and J. Chazelas, *Phys. Rev. Lett.* **61**, 2472 (1988).
- ²M. Julliere, *Phys. Lett.* **54A**, 225 (1975).
- ³S. Maekawa and U. Gäßvert, *IEEE Trans. Magn.* **18**, 707 (1982).
- ⁴T. Miyazaki and N. Tezuka, *J. Magn. Magn. Mater.* **139**, L231 (1995); **151**, 403 (1995); *J. Magn. Soc. Jpn.* (in Japanese) **21**, 493 (1997); *J. Appl. Phys.* **79**, 6262 (1996).
- ⁵J. S. Moodera, L. R. Kinder, T. M. Wong, and R. Meservey, *Phys. Rev. Lett.* **74**, 3273 (1995); J. S. Moodera, L. R. Kinder, J. Nowak, P. LeClair, and R. Meservey, *Appl. Phys. Lett.* **69**, 708 (1996); J. S. Moodera and L. R. Kinder, *J. Appl. Phys.* **79**, 4724 (1996); **81**, 5515 (1997); J. S. Moodera, E. F. Gallagher, K. Robinson, and J. Nowak, *Appl. Phys. Lett.* **70**, 3050 (1997).
- ⁶C. L. Platt, B. Dieny, and A. E. Berkowitz, *Appl. Phys. Lett.* **69**, 2291 (1996); *J. Appl. Phys.* **81**, 5523 (1997).
- ⁷C. Kwon, Q. X. Jia, Y. Fan, M. F. Hundley, D. W. Reagor, J. Y. Coulter, and D. E. Peterson, *Appl. Phys. Lett.* **72**, 486 (1998).
- ⁸C. H. Shang, G. P. Berera, and J. S. Moodera, *Appl. Phys. Lett.* **72**, 605 (1998).
- ⁹R. Meservey and P. M. Tedrow, *Phys. Rep.* **238**, 174 (1994); P. Fulde, *Adv. Phys.* **22**, 667 (1973); *Phys. Rev. B* **7**, 318 (1973); **16**, 4907 (1977).
- ¹⁰J. C. Slonczewski, *J. Phys. (Paris), Colloq.* **49**, C8-1629 (1988); *Phys. Rev. B* **39**, 6995 (1989); *Symposium On Magnetism and Magnetic Materials*, edited by H. L. Huang and P. C. Kuo (World Scientific, Singapore, 1990), pp. 285.
- ¹¹T. Yaoi, S. Ishio, and T. Miyazaki, *J. Magn. Soc. Jpn.* **16**, 303 (1992).
- ¹²J. M. MacLaren, X.-G. Zhang, and W. H. Butler, *Phys. Rev. B* **56**, 11 827 (1997).
- ¹³A. M. Bratkovsky, *Phys. Rev. B* **56**, 2344 (1997).
- ¹⁴S. Maekawa, J. Inoue, and H. Itoh, *J. Appl. Phys.* **79**, 4730 (1996); J. Inoue and S. Maekawa, *Phys. Rev. B* **53**, R11 927 (1996).
- ¹⁵S. T. Chui, *Phys. Rev. B* **55**, 5600 (1997).
- ¹⁶N. F. Schwabe, R. J. Elliott, and N. S. Wingreen, *Phys. Rev. B* **54**, 12 953 (1996).
- ¹⁷R. Y. Gu, D. Y. Xing, and J. M. Dong, *J. Appl. Phys.* **80**, 7163 (1996).
- ¹⁸J. Mathon, *Phys. Rev. B* **56**, 11 810 (1997).
- ¹⁹P. Grünberg, R. Schreiber, Y. Pang, M. B. Brodsky, and H. Sowers, *Phys. Rev. Lett.* **57**, 2442 (1986); *J. Appl. Phys.* **63**, 3473 (1988).
- ²⁰S. S. P. Parkin, N. More, and K. P. Roche, *Phys. Rev. Lett.* **64**, 2304 (1990).
- ²¹P. Bruno and C. Chappert, *Phys. Rev. Lett.* **67**, 1602 (1991); **67**, 2592(E); *Phys. Rev. B* **46**, 261 (1992).
- ²²D. M. Edwards and J. Mathon, *J. Magn. Magn. Mater.* **93**, 85 (1991); D. M. Edwards *et al.*, *Phys. Rev. Lett.* **67**, 493 (1991); *J. Phys.: Condens. Matter* **3**, 4941 (1991).
- ²³J. Barnàs, *J. Magn. Magn. Mater.* **111**, L215 (1992).
- ²⁴R. P. Bruno, *Europhys. Lett.* **23**, 615 (1993).
- ²⁵S. N. Okuno and K. Inomata, *Phys. Rev. Lett.* **72**, 1553 (1994); *Phys. Rev. B* **51**, 6139 (1995); K. Inomata *et al.*, *J. Magn. Magn. Mater.* **156**, 219 (1996).
- ²⁶P. J. H. Bloemen, M. T. Johnson, M. T. H. van de Vorst, R. Coehoorn, J. J. de Vries, R. Jungblut, J. aan de Stegge, A. Reinders, and W. J. M. de Jonge, *Phys. Rev. Lett.* **72**, 764 (1994).
- ²⁷P. Bruno, *J. Magn. Magn. Mater.* **121**, 248 (1993); *Phys. Rev. B* **49**, 13 231 (1994); **52**, 411 (1995).
- ²⁸A. Vedyayev, N. Ryzhanova, C. Lacroix, L. Giacomoni, and B. Diny, *Europhys. Lett.* **39**, 219 (1997).
- ²⁹W.-S. Zhang and B.-Z. Li, *Chin. Phys. Lett.* **15**, 296 (1998); *J. Appl. Phys.* **83**, 5332 (1998).
- ³⁰Y. Li, B.-Z. Li, W.-S. Zhang, and D.-S. Dai, *Phys. Rev. B* **57**, 1079 (1998); *Chin. Phys. Lett.* **15**, 210 (1998).
- ³¹X. Zhang, B.-Z. Li, W.-S. Zhang, and F.-C. Pu, *Phys. Rev. B* **57**, 1090 (1998).
- ³²M. B. Stearns, *J. Magn. Magn. Mater.* **5**, 167 (1977).
- ³³C. B. Duke, *Tunneling in Solids* (Academic, New York, 1969); in *Tunneling Phenomena in Solids*, edited by E. Burstein and S. Lundquist (Plenum, New York, 1969), pp. 31.
- ³⁴R. P. Erickson, K. B. Hathaway, and J. R. Cullen, *Phys. Rev. B* **47**, 2626 (1993); *J. Magn. Magn. Mater.* **104-107**, 1840 (1992).
- ³⁵D. M. Edwards, J. M. Ward, and J. Mathon, *J. Magn. Magn. Mater.* **126**, 380 (1993); D. M. Edwards *et al.*, *ibid.* **140-144**, 517 (1995).
- ³⁶V. Drchal, J. Kudrnovsky, I. Turek, and P. Weinberger, *Phys. Rev. B* **53**, 15 036 (1996).
- ³⁷J. Barnàs and Y. Bruynseraede, *Phys. Rev. B* **53**, R2956 (1996).
- ³⁸D. Li, J. Pearson, S. D. Bader, E. Vescovo, D.-J. Huang, P. D. Johnson, and B. Heinrich, *Phys. Rev. Lett.* **78**, 1154 (1997).